Surface Modification of Exfoliated Layered Gadolinium Hydroxide for the Development of Multimodal Contrast Agents for MRI and Fluorescence Imaging

By *Young-su Yoon, Byung-Il Lee, Kyung Sig Lee, Geun Ho Im, Song-Ho Byeon,* Jung Hee Lee,** and *In Su Lee**

A novel method for modifying the surface of magnetic-resonance-contrasting layered gadolinium hydroxide (LGdH) is developed providing them with water- and bio-compatibility and acid-resistance, all of which are essential for medical applications. A stable colloid of exfoliated layers is synthesized by exchanging interlayer anions of LGdH with oleate ions. The delaminated layers are successively coated with phospholipids with poly(ethylene glycol) tail groups, and their effectiveness as a contrast agent for magnetic resonance imaging (MRI) is demonstrated. The adaptability of this surface modification approach for incorporating functional molecules and fabricating a fluorescent colloid of LGdH, which has the potential utility as a multimodal probe, is also demonstrated. This result provides a novel approach for expanding the applications of layered inorganic materials and developing a new class of MRI contrast agents.

1. Introduction

Layered rare-earth hydroxides (LRHs) are a class of anionic clays that are composed of positively charged hydroxide layers of trivalent rare-earth ions, but are otherwise structurally similar to hydrotalcite-type layered double hydroxides (LDHs).[1] This series of LRHs with a general composition of $RE_2(OH)_5X \cdot nH_2O$ (RE = rare-earths, X = anions) has been recently synthesized and is attracting increasing attention on account of their unique ability to combine the useful properties of rare-earth ions with the host–guest chemistry of LDHs.[2] The magnetic resonance (MR) relaxation properties of layered gadolinium hydroxide (LGdH) were previously examined, and its potential utility as a positive contrast agent for MRI was proposed in our previous report.[3] The major potential advantage of using LGdH as a contrast agent is that it can be delaminated to expose most of the MR-active Gd^{3+} ions at the water-accessible surface, and therefore, operate at a low dose of contrast agent. Furthermore, LGdH can also incorporate functional molecules between the hydroxide layers, providing a multifunctional system that combines MR imaging (MRI) with other clinical treatments.[4,5] However, many significant challenges remain to be overcome before LGdH can be applied clinically. These include: 1) remaining in the bloodstream for a long time while retaining its high-contrast efficiency, which requires a stable dispersion of completely exfoliated layers; 2) reducing the nonspecific adhesive binding to the cellular membrane, which obstructs target-specific imaging; 3) improving the stability in the low pH environment of a physiological suspension.

In this context, this study developed a method for modifying the surface of LGdH layers providing them with water- and bio-compatibility and acid-resistance. Recently, several surface modification methods of rendering LDH layers that are stably dispersible in a colloidal suspension have been reported.[6,7] However, most of them were carried out in an organic solvent system, and moreover, the method for conferring water-dispersity to LDH-type compounds remains an important challenge.[8] In this study, the nitrate ion of $Gd_2(OH)_5NO_3 \cdot nH_2O$ was first exchanged with the oleate anion, which is one of the well-known dispersion agents in nonpolar solvents, to disperse the LGdH layers into an organic suspension. The delaminated layers were then modified with phospholipids with poly(ethylene glycol) (PEG) tail groups, resulting in a stable aqueous suspension of completely exfoliated layers having an ability for enhancing MRI contrast. Fluorescein anions were incorporated into the modified layers using the ready exchange of anions attached to an exfoliated layer forming a fluorescent colloid of LGdH, which may allow the development of a multimodal probe combining optical and MR imaging (Scheme 1).[9] This paper reports this novel surface modification method, which results in a fluorescent colloid of LGdH layers that are completely exfoliated and stably dispersed in aqueous media. Their well-directed characteristics as a contrast agent for MRI with practical applications in medicine are also demonstrated.

[*] Prof. S.-H. Byeon, Prof. I. S. Lee, Y.-S. Yoon, B.-I. Lee, K. S. Lee
Department of Applied Chemistry, College of Applied Science
Kyung Hee University
Gyeonggi-do 446-701 (Korea)
E-mail: shbyun@khu.ac.kr; insulee97@khu.ac.kr
Prof. J. H. Lee, G. H. Im
Department of Radiology, Samsung Medical Center
Sungkyunkwan University School of Medicine
Seoul 135-710 (Korea)
E-mail: hijunghee@skku.edu

DOI: 10.1002/adfm.200901051

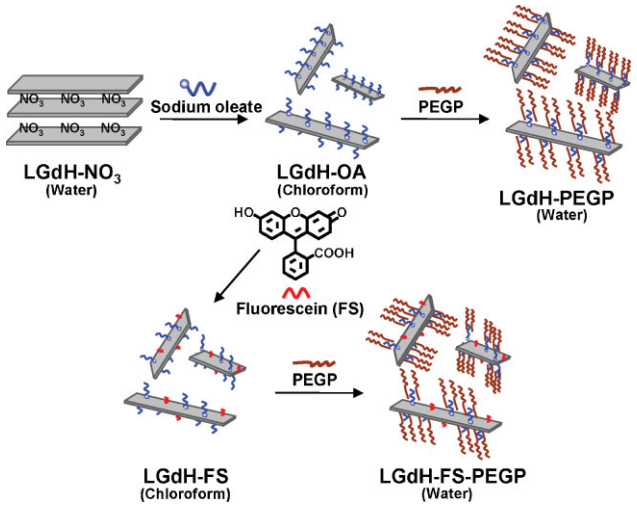

Scheme 1. The surface modification approach for the fabrication of **LGdH-FS-PEGP**.

2. Results and Discussion

2.1. Surface Modification and Characterization

LGdH with the chemical formula of $Gd_2(OH)_5NO_3 \cdot nH_2O$ ($n \approx 1.0$) (**LGdH-NO$_3$**) was prepared using a previously reported procedure comprising the hydrothermal reaction of a Gd^{3+}-containing aqueous solution.[2a] The aqueous suspension of **LGdH-NO$_3$** has insufficient colloidal stability, in which the powder settles immediately after shaking the suspension. In the first step of surface modification, the aim was to exchange the interlayer NO_3^- anions with oleate by adding **LGdH-NO$_3$** in an aqueous solution containing sodium oleate, and then reacting it at room temperature for 24 h. The X-ray diffraction (XRD) pattern of the resulting powder showed a series of strong (00*l*) reflections, which are characteristic of layered compounds (Fig. 1a). The interlayer spacing was expanded from 0.85 to 4.6 nm after the ion-exchange reaction, suggesting an intercalation of long-chain oleate anions in the interlayer of LGdH. The IR spectrum of the pristine **LGdH-NO$_3$** showed a sharp band corresponding to the ν_3 mode of the nitrate ion at around 1384 cm^{-1}. Such a band was not observed in the IR spectrum of oleate-exchanged LGdH. The intense bands at around 1558 and 1458 cm^{-1} are assigned to $\nu_{as}(COO^-)$ and $\nu_s(COO^-)$, respectively (Fig. 1b). This difference in IR spectra supported a successful exchange of NO_3^- with the oleate units in the interlayer gallery of LGdH. Thermogravimety (TG) and elemental analysis (EA) confirmed the complete replacement of NO_3^- in the host and the intercalation of oleate anions and oleic acid generating $Gd_2(OH)_5(oleate)(oleic\ acid)_{0.63} \cdot 1.5H_2O$ (**LGdH-OA**). Due to strong lateral dispersion interactions between long-chain alkyl ions, the intercalation of excess neutral carboxylic acid was also observed with decanoic acid in a previous study.[2a] When this powder was dispersed in a nonpolar organic solvent, such as toluene or chloroform, the **LGdH-OA** layers were readily delaminated. The generated stable colloidal suspension exhibited a clear Tyndall light scattering effect under laser illumination (Fig. 1c). Atomic force microscopy (AFM) analysis of the deposits left by the **LGdH-OA** suspension on the substrate revealed the dispersion of ultrathin nanosheets with a mean thickness and lateral size of 4.0(±0.4) and 130(±60) nm, respectively (Fig. 1d). The layer thickness observed in the AFM image was comparable with that of a monolayer with oleate anions at the surface, which was expected from the interlayer spacing of **LGdH-OA**, confirming the exfoliation of the layers.

In order to provide the layers with water- and bio-compatibility, the exfoliated layers of **LGdH-OA** were modified with a PEG-phospholipid, producing a nonpolar surface coated with a shell of nontoxic, nonimmunogenic, nonantigenic, and protein-resistant PEG chains.[10] The surface coating was applied by mixing PEG-phospholipid and **LGdH-OA** in a $CHCl_3$ suspension, evaporating the solvent, and completely drying in vacuo.[11] The addition of water followed by filtering off any floating material generated a translucent colloidal suspension of delaminated LGdH layers. Purification of the PEG-phospholipid-modified LGdH (**LGdH-PEGP**) was carried out by repetitions of ultracentrifugation

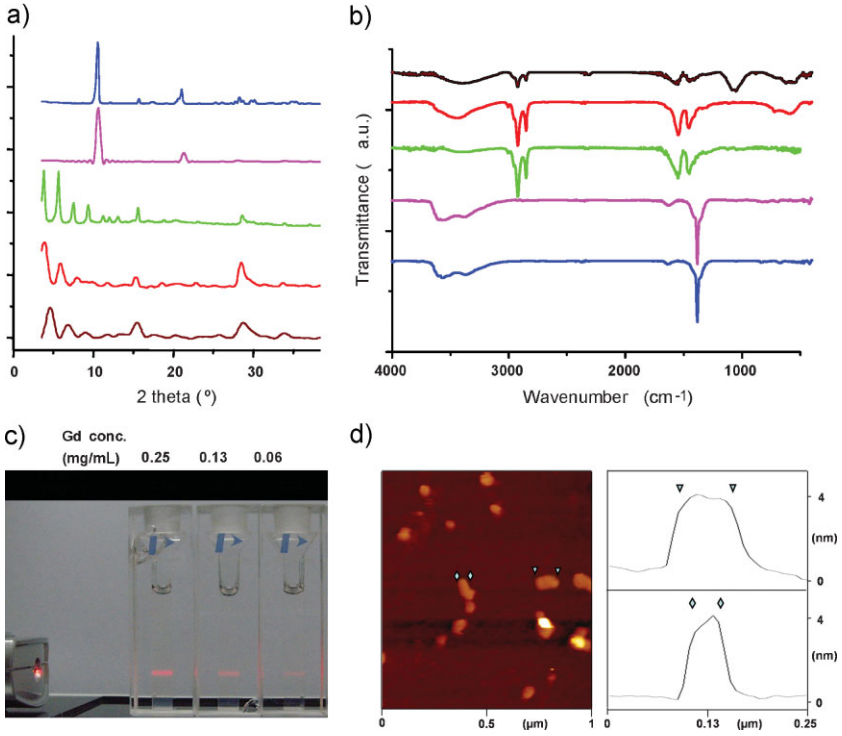

Figure 1. a) XRD and b) IR spectra of **LGdH-NO$_3$** (blue), **LGdH-NO$_3$** treated with fluorescein sodium salt in an aqueous suspension (pink), **LGdH-OA** (green), **LGdH-FS** (red), and resulting adduct of the reaction between **LGdH-OA** and excess of fluorescein free acid (brown). c) Photographs of the **LGdH-OA** suspension in $CHCl_3$ showing the Tyndall effect. d) AFM image of the **LGdH-OA** layers randomly chosen from a deposit of the colloid in $CHCl_3$.

followed by redispersion in water. The resulting **LGdH-PEGP** exhibited good colloidal stability in aqueous suspension. Laser illumination of the aqueous **LGdH-PEGP** suspensions demonstrated the Tyndall scattering effect, which confirmed the generation of a colloidal suspension (Fig. 2a).

For further development of the current modification method, fluorescent molecules were incorporated into the modified layers to give an additional functionality. In order to employ the ready exchange of anions at the surface of the exfoliated layers, **LGdH-OA** was added to a mixture of CH_3Cl/CH_3OH (in 7:3 ratio) containing fluorescein free acids and a small amount of triethylamine, and the reaction was carried out at room temperature for 12 h. The use of excess fluorescein rapidly replaced most of the oleate and oleic acid of **LGdH-OA** with fluorescein anions, generating a precipitate with poor dispersibility during the reaction. In order to incorporate fluorescein while retaining the sufficient colloidal stability, only a small amount of fluorescein acid (2 mg) was reacted with **LGdH-OA** (100 mg), which was then isolated by repeated ultracentrifugation and washing with the CH_3Cl/CH_3OH mixture. The resulting LGdH powder carrying a small amount of fluorescein (**LGdH-FS**) was readily dispersed in an organic solvent, generating a fluorescent colloid of exfoliated layers (Fig. 2b,c). The emission spectra of **LGdH-FS** showed a slight blue-shift of its fluorescent band compared with that of the free fluorescein molecule (Fig. 2d). The amount of fluorescein molecules incorporated in **LGdH-FS**, as determined by the amount of fluorescein remaining after the exchange reaction, was 2.5×10^{-3} mole per 1 mole of Gd ions of LGdH. When **LGdH-NO_3** was reacted with a fluorescein sodium salt in an aqueous suspension for a control experiment, there was no displacement of interlayer NO_3^- anions. Inability of fluoresceins to direct exchange in the interlayer space explains the necessity of layer exfoliation for the fluorescent modification of LGdH layers by fluorescein exchange. Treatment of the exfoliated layers of **LGdH-FS** with PEG-phospholipid resulted in an aqueous colloid of LGdH, which incorporated fluorescein and was encapsulated by a PEG shell (**LGdH-FS-PEGP**) (Fig. 3a,b). AFM analysis of the deposits left by the **LGdH-FS-PEGP** suspension on the substrate revealed the dispersion of ultrathin nanosheets with a mean thickness and lateral size of 6(±1) and 130(±60) nm, respectively, confirming the exfoliation of the layers (Fig. 3c). The illumination of the **LGdH-FS-PEGP** suspensions with 365 nm excitation light exhibited a green fluorescence, demonstrating its utility as an optical probe.

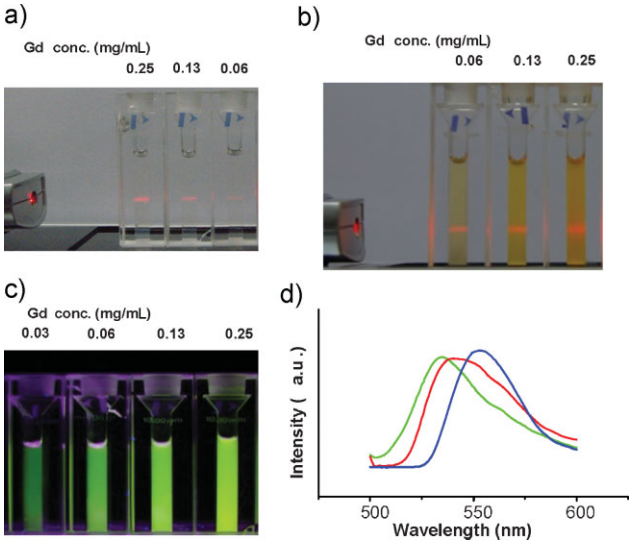

Figure 2. Photographs of a) the aqueous suspension of **LGdH-PEGP** and b) the $CHCl_3$ suspension of **LGdH-FS** showing the Tyndall effect. c) Photographs of the CH_3Cl suspension of **LGdH-FS** showing the fluorescence under 365 nm excitation light. (d) Fluorescence spectra of the **LDH-FS** (green) and fluorescein free acid (red) in $CHCl_3/CH_3OH$ mixture solvent, and fluorescein sodium salt in water (blue) with the excitation at 490 nm.

2.2. Evaluation of Effectiveness as a MRI Contrast Agent

The colloidal suspensions of **LGdH-FS-PEGP** exhibited excellent stability, which is essential for biomedical applications. Indeed, no sedimentation was detected when the suspension was left standing for more than a month at room temperature. The stability of **LGdH-FS-PEGP** was also examined in buffer suspensions at various pH. The supernatant solutions isolated after treatment at pH 4.6 and 3.0 for 12 h showed 3 and 8% dissolution of **LGdH-FS-PEGP**, respectively. If we consider that the LGdH before modification showed 33 and 50% dissolution at pH 4.6 and 3.0, respectively, within 1 h,[3] such a significantly lower ratio of dissolution illustrates greatly enhanced acid-resistance by the surface modification. The in-vitro cytotoxicity was evaluated on MCF-7 cells using the MTT ([3-(4,5-dimethylthiazol-2-yl)-2,5-diphenyltetrazolium bromide]) method.[12] **LGdH-FS-PEGP** had no significant cytotoxic effects up to a Gd concentration of 10 μM (Fig. 4). In order to evaluate the effectiveness of **LGdH-FS-PEGP** as an MRI contrast agent, the relaxation properties of its suspensions were examined using a 3.0 T human clinical scanner. LGdH was found to decrease both the longitudinal relaxation time (T_1) and transverse relaxation time (T_2). Accordingly, bright and dark signal enhancement was observed in the T_1- and T_2-weighted images, respectively (Fig. 5a). The specific relaxivity of **LGdH-FS-PEGP**, which was determined by measuring the relaxation rates as a function of the Gd concentration, were 1.72 and 31.56 s^{-1} mM^{-1} for r_1 and r_2, respectively (Fig. 5b). The r_2 value of **LGdH-FS-PEGP** was enhanced considerably while its r_1 value was slightly lower than that of the unmodified LGdH.[3] Although the exact explanation for their relaxation properties requires further research, the enhancement of r_2 can be explained by considering the increased surface of the exfoliated layers, which generate field gradients through which water molecules diffuse. The reduced r_1 can be attributed to the low permeability of water molecules through the surfactant shell surrounding the LGdH layer and consequent decrease of the water exchange rate. Such a relaxation phenomenon was previously observed when high concentrations of paramagnetic complexes, such as Gd^{3+} or Dy^{3+}, are entrapped in vesicles such as liposomes.[13] The high r_2/r_1 ratio of 18 for **LGdH-FS-PEGP** suggested that they would be useful as a T_2-contrasting agent for MRI. The contrast efficacy of **LGdH-FS-PEGP** was also observed in an abdominal MRI experiment within a mouse. After intravenous injection of **LGdH-FS-PEGP** layers (2.21 μg of Gd measured by inductively-coupled-plasma–atomic-emission spectroscopy, ICP–AES) into a mouse, a significant

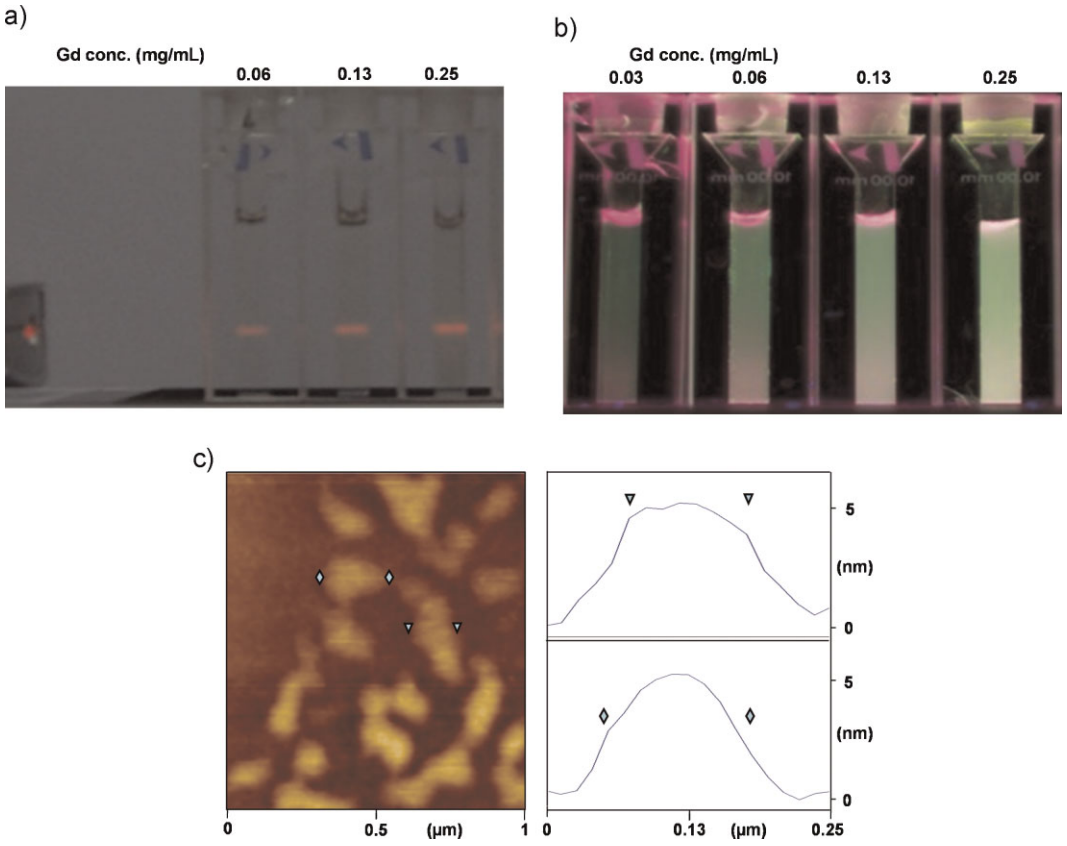

Figure 3. Photographs of the aqueous suspension of **LGdH-FS-PEGP** showing a) the Tyndall effect and b) the fluorescence under 365 nm excitation light. c) AFM image of the **LGdH-FS-PEGP** layers randomly chosen from a deposit of the aqueous colloid.

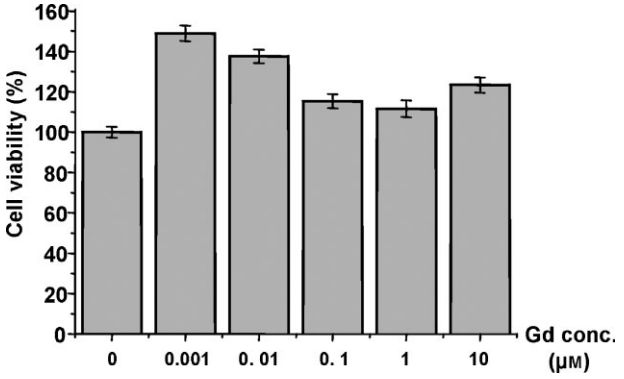

Figure 4. The cytotoxicity of **LGdH-FS-PEGP** to MCF-7 cells as a function of the Gd concentration. The results are presented as the mean of four experiments with standard deviations.

signal loss was induced in the T_2-weighted MRI of the abdomen. The spleen and liver were shown dark in the MRI due to the injected **LGdH-FS-PEGP**, which was observed throughout the experiment (Fig. 6).

3. Conclusion

In conclusion, a novel method for modifying the surface of MR contrasting LGdH layers was developed; the modifications provides them with water- and bio-compatibility and acid-resistance, which are essential for medical applications. A stable colloid of exfoliated LGdH layers was synthesized using the newly developed surface modification method, and their effectiveness as a contrast agent for MRI was demonstrated. The adaptability of this surface modification approach for incorporating functional molecules and fabricating a fluorescent colloid of LGdH, which has the potential utility as a multimodal probe, was also demonstrated. It is believed that this result provides a novel approach for expanding the applications of layered inorganic materials and developing a new class of MRI contrast agents.

4. Experimental

General Considerations: All reagents, including $GdCl_3 \cdot 6H_2O$ (Aldrich), sodium oleate (TCI), oleic acid (Aldrich), the phthalate buffer (pH 4.6, Samchun Chem.), and 1,2-distearoyl-sn-glycero-3-phosphoethanolamine-*N*-[methoxypoly(ethylene glycol)-2000] (mPEG-2000 PE, Avanti Polar Lipids, Inc.), were used as purchased without any purification. Transmission electron microscopy (TEM) was conducted with a JEOL JEM-2010. Scanning electron microscopy (SEM) was carried out with a LEO SUPRA 55 (Carl Zeiss, Germany). XRD were obtained by using a rotating-anode-installed X-ray diffractometer (18 kW) (Mac Science, Japan). AFM was carried out by using a Pucostation STD (Pucostation). TG analysis was done using a TG/DTA320 SSC/5200 S11 system (Seiko instruments). UV absorption and fluorescence were observed using a V670 UV–visible–NIR spectrophotometer (JASCO) and FP-6600 spectrofluorometer (JASCO), respectively.

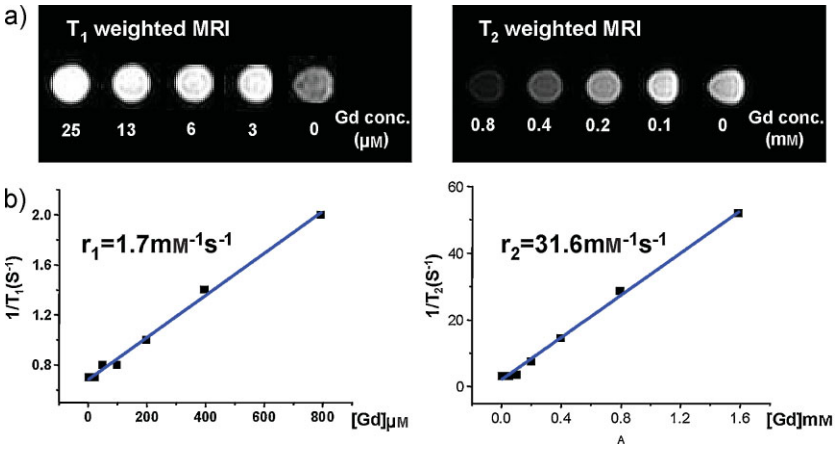

Figure 5. a) T_1- and T_2-weighted MRIs obtained from aqueous suspensions of **LGdH-FS-PEGP**. Plots of b) T_1^{-1} and T_2^{-1} versus Gd concentration of **LGdH-FS-PEGP**.

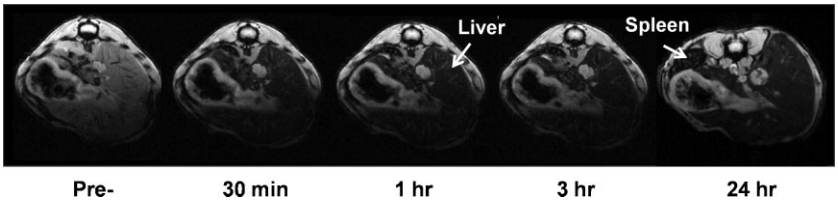

Figure 6. T_2-weighted MRI of mouse body. The signal drop in the liver and spleen is significant by **LGdH-FS-PEGP** (10 mg kg^{-1} of body weight) injected intravenously.

*Synthesis of **LGdH-OA***: **LGdH-NO$_3$** was prepared by the method described previously with some modifications [2a]. **LGdH-NO$_3$** (2.00 g) was dispersed in an aqueous solution (100 mL) containing sodium oleate (4.00 g) and stirred at room temperature for 24 h. The resulting **LGdH-OA** was isolated by filtration and washed with water several times. The chemical formula of **LGdH-OA**, $Gd_2(OH)_5(C_{17}H_{33}CO_2)(C_{17}H_{33}CO_2H)_{0.63} \cdot 1.5H_2O$, was determined using EA and TG. Observed values of 40.13 and 7.32% for C and H, respectively, are well in agreement with the calculated values based on the formula (39.78 and 7.10%). The %N was not detected by EA, indicating the complete exchange of nitrate ions by oleate and oleic acids. A weight loss of 3.32% was observed below 200 °C during TG analysis, which is close to the calculated weight percentage, 3.05%, of co-intercalated water molecules in the formula. The composition of $Gd_2(OH)_5(C_{17}H_{33}CO_2)(C_{17}H_{33}CO_2H)_{0.63} \cdot 1.5H_2O$, was also supported by the 59.23% total ignition loss, which is close to the calculated loss of 59.08% (Fig. 7).

*Synthesis of **LGdH-PEGP***: **LGdH-OA** (30 mg) was mixed with PEG-phospholipid (90 mg) in a $CHCl_3$ suspension and stirred at room temperature for 30 min. The solvent was evaporated by using a rotary evaporator and completely removed in vacuo. The water (50 mL) was added to the reaction mixture, and the suspension was filtered through a membrane filter with a pore diameter of 800 nm. The resulting **LGdH-PEGP** was isolated by repeated ultracentrifugation and redispersion in distilled water.

*Reaction of **LGdH-NO$_3$** with Fluorescein Sodium Salt*: **LGdH-NO$_3$** (30 mg) was dispersed in an aqueous solution (50 mL) containing fluorescein sodium salt (300 mg) and stirred at 25 °C for 12 h. The precipitate generated from the reaction was obtained by filtration and washed with water several times.

*Synthesis of **LGdH-FS***: **LGdH-OA** (30 mg) was added to a CH_3Cl/CH_3OH (in 7:3 ratio) suspension (50 mL) containing fluorescein free acid (0.6 mg) and triethylamine (20 μL) and stirred at room temperature for 30 min. The resulting solid of **LGdH-FS** was isolated by repeated ultracentrifugation and washing with CH_3Cl/CH_3OH.

*Synthesis of **LGdH-FS-PEGP***: **LGdH-FS** (30 mg) was mixed with PEG-phospholipid (90 mg) in a $CHCl_3$ suspension and stirred at room temperature for 30 min. The solvent was evaporated using a rotary evaporator and completely removed in vacuo. Water (50 mL) was added to the reaction mixture, and the suspension was filtered through a membrane filter with an 800 nm pore diameter. The targeted **LGdH-FS-PEGP** was isolated by repeated ultracentrifugation and redispersion in distilled water.

Stability Evaluation under Acidic Environment: In order to examine the stability in acidic solution, **LGdH-FS-PEGP** containing 0.6 mg of Gd were dispersed in 1 mL of a phthalate buffer solution at pH 7.0, 6.0, 4.6, and 3.0 and stirred at room temperature. After 0, 1, 2, 4, and 12 h, 100 μL of each suspension were collected and centrifuged to remove the **LGdH-FS-PEGP** solids. The amount of Gd in the supernatant solution for each time was determined by ICP analysis.

*Cytotoxicity Evaluation of **LGdH-FS-PEGP***: Cell viability was determined in MCF-7 cells maintained in growth media (RPMI 1640 and Leibovitz's L-15 media with L-glutamin, 1% antibiotic-antimycotic, 10% fetal bovine serum) at 37 °C in a humidified atmosphere of 5% CO_2. Cytotoxicity of LGdH was evaluated by measuring the inhibition of cell growth using the MTT assay [11]. Cells were plated at a density of 5 cells × 103 cells mL^{-1} in 96-well plates and treated with the above compounds for 72 h. After treatment, the cells were washed and incubated for an additional 0.5 mg of MTT for 3 h. Cell viabilities were presented as the ratio of the number of cells treated to the number of nontreated control cells. Cell viability graphs were plotted as Gd concentration.

Measuring MRI Relaxation Properties: T_1 and T_2 relaxation times of **LGdH-FS-PEGP**, which were prepared in test tubes with varying concentrations were measured on a 3.0 T clinical MRI scanner (Philips, Achieva ver. 1.2, Philips Medical Systems, Best, The Netherlands) with an 80 mT m^{-1} gradient amplitude and a 200 ms m^{-1} slew rate. All measurements were carried out around pH 7. A Look–Locker sequence (relaxation time (TR)/echo time (TE) = 10/1 ms and flip angle = 5) was used to measure T_1 by acquiring 17 gradient echo images at different inversion delay times using a minimum inversion time of 87 ms with a

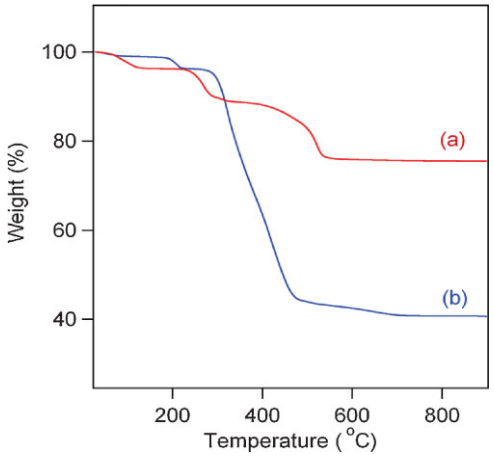

Figure 7. TG analysis curves of a) **LGdH** and b) **LGdH–OA**.

phase interval of 264 ms with an in-plane image resolution of 625 mm × 625 mm^2 and a slice thickness of 500 mm. The images were fitted into a three-parameter function to calculate T_1 values using the Matlab program. T_2 measurements were performed by using 10 different echo times in a multislice turbo spin echo sequence (TR/TE = 5000/20, 40, 60, 80, 100, 120, 140, 160, 180, and 200 ms; in-plane resolution = 200 mm × 200 mm^2; slice thickness = 500 mm). The images were fitted using the Levenberg–Marquardt method to calculate T_2 values using the Matlab program. We calculated the specific relaxivities (r_1 and r_2) of the nanoparticles from the plot of T_1^{-1} and T_2^{-1} versus concentration of contrast agent. The signal intensities of each of the regions of interest in the T_1 map (60–80 pixels) and the T_2 map (200–300 pixels) were measured for each concentration, which were then used for r_1 and r_2 calculations, respectively.

Mouse in vivo MRI: Six C3H mice weighing 25–35 g were employed under the institutional guidelines of the Samsung Biomedical Research Institute for animal handling. For an intravascular delivery of **LGdH-FS-PEGP**, 10 mg of Gd (measured by ICP–AES) per kilogram of mouse body weight was administered through a tail vein of a mouse. For in vivo MRI, the animals were anesthetized and set into an MR-compatible cradle. During MRI, the animals were anesthetized by inhaling oxygen-enriched air with 2% isoflurane via a facemask. The rectal temperature was carefully monitored and maintained at 36 ± 1 °C. To investigate the time course of distribution of the hollow manganese oxide nanoparticles (HMON) in the mouse, MRI was performed before and after (3, 24, 48, and 72 h; and 7 days) administration of HMON for three animals. All in vivo MRI were carried out on a 7T/20 MRI System (Bruker-Biospin, Fallanden, Switzerland) equipped with a 20 cm gradient set capable of supplying up to 400 mT m^{-1} in a 100 μsec rise-time. A birdcage coil (72 mm i.d.) (Bruker-Biospin, Fallanden, Switzerland) was used for excitation, and an actively decoupled phased array coil was used for receiving the signal. High-resolution HMON contrast-enhanced multislice MR images were obtained for each mouse brain using a fast spin-echo T_1-weighted MRI sequence (TR/TE = 300/7.9 ms, number-of-experiments (NEX) of 4, echo train length of 2, an in-plane resolution of 100 μm × 100 μm with a slice thickness of 800 μm and 10 slices) and a fast spin-echo T_2-weighted MRI sequence (TR/TE = 3000/60 ms, NEX = 4, echo train length = 4, an in-plane resolution of 100 μm × 100 μm with a slice thickness of 800 μm and 10 slices).

Acknowledgements

This work was supported by a Korea Research Foundation Grant funded by the Korean Government (MOEHRD) (KRF-2008-314-C00192) (S. H. B. and I. S. L.) and by the Samsung Biomedical Research Institute grant (C-A8-224 and OTX1070221) (J. H. L).

Received: June 14, 2009
Revised: July 29, 2009
Published online: September 9, 2009

[1] a) M. Louer, D. Louer, A. L. Delgado, O. G. Martinez, *Eur. J. Inorg. Chem.* **1989**, *26*, 241. b) D. Louer, M. Louer, *J. Solid State. Chem.* **1987**, *68*, 292. c) J. M. Haschke, *Inorg. Chem.* **1974**, *13*, 1812.

[2] a) K.-H. Lee, S.-H. Byeon, *Eur. J. Inorg. Chem.* **2009**, 929. b) L. J. McIntyre, L. K. Jackson, A. M. Fogg, *Chem. Mater.* **2008**, *20*, 335. c) F. Geng, Y. Matsushita, R. Ma, H. Xin, M. Tanaka, F. Izumi, N. Iyi, T. Sasaki, *J. Am. Chem. Soc.* **2008**, *130*, 16344. d) F. Gandara, J. Perles, N. Snejko, M. Iglesias, B. Gomez-Lor, E. Gutierrez-Puebla, M. A. Monge, *Angew. Chem. Int. Ed.* **2006**, *45*, 7998.

[3] B.-I. Lee, K. S. Lee, J. H. Lee, I. S. Lee, S.-H. Byeon, *Dalton Trans.* **2009**, 2490.

[4] a) Z. Gu, A. C. Thomas, Z. P. Xu, J. H. Campbell, G. Q. Lu, *Chem. Mater.* **2008**, *20*, 3715. b) Z. P. Xu, N. D. Kurniawan, P. F. Barlett, G. Q. Lu, *Chem. Eur. J.* **2007**, *13*, 2824. c) L. Desigaux, M. B. Belkacem, P. Richard, J. Cellier, P. Léone, L. Cario, F. Leroux, C. Taviot-Guého, B. Pitard, *Nano Lett.* **2006**, *6*, 199. d) F. Leroux, C. Taviot-Guého, *J. Mater. Chem.* **2005**, *15*, 3628. e) S.-Y. Kwak, W. M. Kriven, M. A. Wallig, J.-H. Choy, *Biomaterials* **2004**, *25*, 5995. f) A. I. Khan, L. Lei, A. J. Norquist, D. O'Hare, *Chem. Commun.* **2001**, 2342. g) J. H. Choy, S. Y. Kwak, Y. J. Jeong, J. S. Park, *Angew. Chem. Int. Ed.* **2000**, *39*, 4042.

[5] a) J. Kim, J. E. Lee, S. H. Lee, J. H. Yu, J. H. Lee, T. G. Park, T. Hyeon, *Adv. Mater.* **2008**, *20*, 478. b) J. Yang, C.-H. Lee, H.-J. Ko, J.-S. Suh, H.-G. Yoon, K. Lee, Y.-M. Huh, S. Haam, *Angew. Chem. Int. Ed.* **2007**, *46*, 8836. c) N. Nasongkla, E. Bey, J. Ren, H. Ai, C. Khemtong, J. S. Guthi, S.-F. Chin, A. D. Sherry, D. A. Boothman, J. Gao, *Nano Lett.* **2006**, *6*, 2427.

[6] For the recent review on the exfoliation of LDH: R. Ma, Z. Liu, L. Li, N. Iyi, T. Sasaki, *J. Mater. Chem.* **2006**, *16*, 3809.

[7] a) S. Ida, D. Shiga, M. Koinuma, Y. Matsumoto, *J. Am. Chem. Soc.* **2008**, *130*, 14038. b) Q. Wu, A. O. Sjåstad, Ø. B. Vistad, K. D. Knudsen, J. Roots, J. S. Pedersend, P. Norby, *J. Mater. Chem.* **2007**, *17*, 965. c) Z. Liu, R. Ma, M. Osada, N. Iyi, Y. Ebina, K. Takada, T. Sasaki, *J. Am. Chem. Soc.* **2006**, *128*, 4872. d) G. Hu, N. Wang, D. O'Hare, J. Davis, *Chem. Commun.* **2006**, 287. e) Q. Wu, A. O. Sjåstad, Ø. B. Vistad, J. Roots, P. Norby, *J. Mater. Chem.* **2005**, *15*, 4695. f) L. Li, R. Ma, Y. Ebina, N. Iyi, T. Sasaki, *Chem. Mater.* **2005**, *17*, 4386. g) M. Singh, M. I. Ogden, G. M. Parkinson, C. E. Buckley, J. Connolly, *J. Mater. Chem.* **2004**, *14*, 871. h) S. O' Leary, D. O'Hare, G. Seeley, *Chem. Commun.* **2002**, 1506.

[8] a) Z. P. Xu, G. S. Stevenson, C.-Q. Lu, G. Q. Lu, P. F. Bartlett, P. P. Gray, *J. Am. Chem. Soc.* **2006**, *128*, 36. b) C. Jaubertie, M. J. Holgado, M. S. San Roman, V. Rives, *Chem. Mater.* **2006**, *18*, 3114. c) T. Hibino, M. Kobayashi, *J. Mater. Chem.* **2005**, *15*, 653.

[9] a) S. Wang, B. R. Jarrett, S. M. Kauzlarich, A. Y. Louie, *J. Am. Chem. Soc.* **2007**, *129*, 3848. b) W. J. Riter, J. S. Kim, K. M. L. Taylor, H. An, W. Lin, T. Tarrant, W. Lin, *Angew. Chem. Int. Ed.* **2007**, *46*, 3680. c) J.-H. Lee, Y.-S. Jun, S.-I. Yeon, J.-S. Shin, J. Cheon, *Angew. Chem. Int. Ed.* **2006**, *45*, 8160. d) W. J. M. Mulder, R. Koole, R. J. Brandwijk, G. Storm, P. T. K. Chin, G. Strijkers, C. de Mello Donegá, K. Nicolay, A. Griffioen, *Nano Lett.* **2006**, *6*, 1.

[10] J. M. Harris, *Poly(ethylene glycol) Chemistry, Biotechnical and Biomedical Applications*, Plenum Press, New York **1992**.

[11] B. Dubertret, P. Skourides, D. J. Norris, V. Noireaux, A. H. Brivanlou, A. Libchaber, *Science.* **2002**, *298*, 1759.

[12] a) T. Mosmann, *J. Immunol. Methods* **1983**, *65*, 55. b) D. Gerlier, N. Thomasset, *J. Immunol. Methods* **1986**, *94*, 57.

[13] a) D. D. Castelli, E. Gianolio, S. G. Crich, E. Terreno, S. Aime, *Coord. Chem. Rev.* **2008**, *252*, 2424. b) S. L. Fossheim, A. K. Fahlvik, J. Klaveness, R. N. Muller, *Magn. Reson. Imaging* **1999**, *17*, 83. c) S. L. Fossheim, K. E. Kellar, A. H. Fahlvik, J. Klaveness, *Magn. Reson. Imaging* **1997**, *15*, 193.